Effect of Dopant Material on the Performance UV Photodetector Based SnO_2 Thin Films Deposited by Sol-Gel Dip-Coating Method

Kaour Selma[1(✉)] and Rechem Djamil[1,2]

[1] Laboratory of Active Component and Material,
University Larbi Ben M'hidi Oum El Bouagh, Oum El Bouaghi, Algeria
selmakaourl85@gmail.com
[2] Department of Electrical Engineering,
Faculty of Sciences and Applied Sciences,
University Larbi Ben M'hidi Oum El Bouagh, Oum El Bouaghi, Algeria

Abstract. Metal oxide nanomaterials have been attracting growing interest for large domains applications such as gas sensors, photocatalysts, solar cell and UV photodetectors. In this works, the undoped and F, Al, Zn (3 at%) doped SnO_2 thin films were successfully deposited by sol-gel dip coating technique and characterized by X-ray diffraction (XRD), UV–Visible spectroscopy and photoconductivity study. Structural analysis showed that all films are poly-crystalline with tetragonal rutile structure where the crystallite size is calculated by the debye Scherer's formula and it was obtained in the range of 6.49 to 9.33. Optical transmittance spectra of the films showed high transparency (>80%) in the visible range and gap energy values were obtained in the range 3.93 to 3.99. Finally, the variation of photocurrent with voltage and with time has been studied under UV illumination (λ = 365 nm). The high photocurrent is observed using F-doped SnO_2 sample while the film doped with Al had the highest photosensitivity. Current-Voltage characteristics of dark and photo current exhibited linear behavior. The phenomena of photoconductivity in SnO_2 thin films were interpreted by chemisorptions of oxygen molecules on the surface.

Keywords: Metal oxide · Thin films · Sol-gel · Photoconductivity
Photodetectors

1 Introduction

In recent years, the transparent conducting oxide (TCO) such as zinc oxide, indium oxide, cadmium oxide, titanium oxide and tin oxide have attracted much attention because of their unique combination of low electrical resistivity and high optical transparency.

Tin oxide is IV VI_2 compound semiconductors with rutile structure. Thin films of SnO_2 are being studied for several applications such as gas sensor [1], solar cells [2], thin films transistors [3] and UV photodetectors [4]. SnO_2 thin film are attractive for UV photodetectors application because of their unique properties including large band

B. Abdelbaki et al. (Eds.): SMSD 2017, *Proceedings of the Third International Symposium on Materials and Sustainable Development*, pp. 197–205, 2018.
https://doi.org/10.1007/978-3-319-89707-3_24

gap (3.6 a 4 eV) [5, 6] the character n-type conduction [7], large excitonic binding energy of 130 meV [8], stoichiometric structure [9], and high UV absorption rate [10].

UV photodetectors have several applications in the field of biological analysis, environmental, optical communication, flam detection, astronomy lithography and detection of missile [11, 12]. A number of earlier reports showed the performance of UV photodetectors in SnO_2 can be dependent by time and temperature of annealing [4], method deposition and element dopant [13–15].

For enhancing the optoelectronic properties of SnO_2 some elements of group II_B, III_B, and VII_B of the periodic table are being used. Among these elements, Zinc, aluminium and fluorine. Numbers of research groups elaborated and studied structural, optical, and morphological proprieties of Zn, Al, and F doped SnO_2 thin films [16–18]. However, to the best of our knowledge, there are no reported works on SnO_2 thin films based photo-sensor and photoconductor doped with Zn, Al, and F.

In this works, our objective is to determine the influence of Zn, Al, and F atoms, in the constant doping ration, on the structural, morphological, optical properties and the performance of UV photodetectors. Sol-gel dip-coating technique was used to deposit the SnO_2 thin films on cleaned glass.

2 Experiment

2.1 Materials

Tin (II) chloride dihydrate 98% ($SnCl_2{:}2H_2O$), Aluminium trichloride hexahydrate ($AlCl_3{:}6H_2O$), zinc (II) chloride ($ZnCl_2$), fluorine ammonium (NH_4F), absolute ethanol 99.8% (C_2H_6O) and hydrochloride acid (HCl) were used to preparing undoped, Zn, Al and F doped thin films.

2.2 Preparation and Characterization

The films were prepared by sol-gel dip coating technique on ultrasonically cleaned substrates. The glass substrate was cleaned by acetone, ethanol and deionized water for 10 min in ultrasonic bath and then dried at room temperature. In another hand, the coating solution for undoped SnO_2 thin film was prepared by dissolving Tin (II) chloride dihydrate 98% ($SnCl_2{:}2H_2O$) (0.2 M) in 30 ml of ethanol absolute (C_2H_6O), then a few drops of HCl was added to solution for accelerating the hydrolysis reaction between the precursor and solvent. The homogenous solution was obtained after stirring at 70 °C for 120 min and was kept in a covered for 24 h at room temperature. The film was deposited by the dip-coating technique with speed 60 mm/min. After dip coating process the film was dried 200 °C for 10 min. In order to increase the thickness of the film, the procedure was repeated 10 times and this film was annealed at 550 °C for 2 h. 3% wt Al, Zn and F doped SnO_2 thin films were elaborated under similar experimental conditions with adding ($AlCl_3{:}6H_2O$), ($ZnCl_2$) and (NH_4F) as a source of Al, Zn and F respectively.

X-ray diffraction (XRD, Bruker AXS-8D) with Cu Kα radiation (Cu Kα = 0.1541 nm) was used to study the structural properties, the surface morphology of the films was analysed with atomic force microscopy (A 100-AFM). The optical band gap of samples was performed by UV-Visible spectrophotometer (jasko V-630) in the range (200–1100).

2.3 Measurement of Photoconductivity

SnO_2-based UV photodetectors were fabricated with planar interdigital Ag electrodes. The Keithley source meter was used to measure UV photoresponse under illumination with 4 W, UV lamp available in tow wavelengths: 254 nm, 365 nm (VL- 4LC, vilber lourmat) and equipped. The Keithley was used to measure current-voltage (I-V) characteristics in dark and under UV source of 365 nm wavelength and intensity 350 μW/cm^2.

3 Results

3.1 Structural Analysis

Figure 1 shows the XRD patterns of the undoped, Zn, Al and F doped SnO_2 thin films. As can be seen five diffraction peaks corresponding to (110), (101), (200), (210), (220) direction without any impurity and secondary phase. These spectra confirm that all films have polycrystalline nature with tetragonal rutile structure with a preferred orientation along (110) plane. All diffraction peaks intensity varies with a dopant. The crystallite size (D) can be calculated from the Scherer's equation [19].

$$D = \frac{0.9\lambda}{\beta \cos\theta} \tag{1}$$

Where λ is the X-ray wavelength, β is the full width at half maximum of the XRD peak, θ is the Bragg diffraction angle.

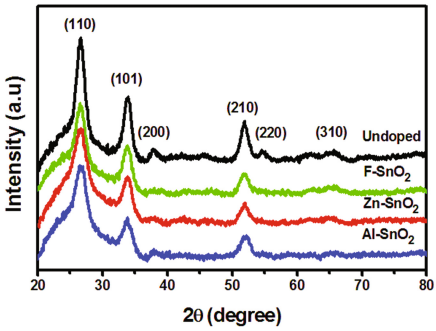

Fig. 1. X-ray Diffractions of the SnO_2 thin films.

The (110) peak was utilized to estimate the crystallite sizes (Table 1). It can be noticed from Table 1 that the crystallite size of the films decreases from 9.33 to 6.49 nm.

Table 1. Data obtained from the XRD and UV–Visible measurement for thin films.

Samples	2θ	FWHM (rad)	Crystalline size (nm)	Gap (eV)
Undoped	26.61	0.016	9.33	3.92
F-SnO_2	26.58	0.018	7.78	3.99
Zn-SnO_2	26.58	0.021	6.79	3.97
Al-SnO_2	26.70	0.023	6.49	3.95

3.2 Optical Properties

The optical transmission spectra of un-doped, fluorine, aluminium and zinc doped tin oxide thin films prepared and deposited by sol-gel dip coating technique on a lime glass substrate and annealed at 550 °C are plotted in Fig. 2a. All films showed high transparency (>80%) in the visible range.

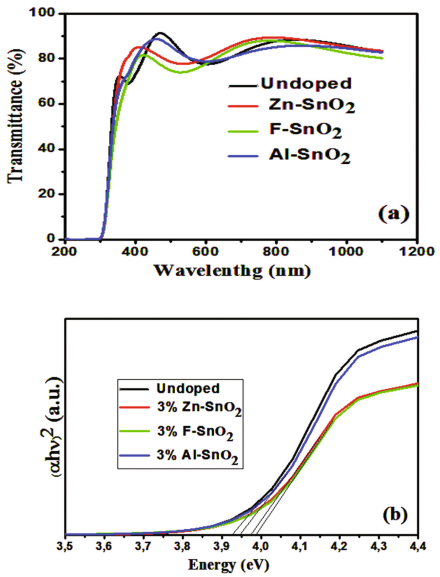

Fig. 2. (a) Optical transmittance spectra of the films, (b) plot of function of photo energy $h\upsilon$ of SnO_2 thin films.

The band gap energy values of different type doped tin oxide thin films were calculated by using the tuc equation [20].

$$\alpha h\upsilon = A(h\upsilon - E_g)^{1/2} \tag{2}$$

Where α The absorption coefficients, A is constant, $h\upsilon$ is photon energy and E_g is the band gap energy.

Figure 2b shows $(\alpha h\upsilon)^2$ variation as a function of photon energy $(h\upsilon)$. The values of optical energy band gap, which was, be estimated from the extrapolating the linear part of $(\alpha h\upsilon)^2$ versus $(h\upsilon)$ plot to $(\alpha h\upsilon)^2$ shown in Table 1. It can be seen that the band-gap energy increased for the all thin films doped with Al, Zn and F. These results are very similar to some reports [21, 22].

3.3 Photoconductivity Study

3.3.1 Voltage Dependence of Dark and Photocurrent

Figure 3 shows a variation of photocurrent and dark current with an applied voltage obtained from undoped as well as Al, Zn and F doped SnO_2 on a log-log scale. From the I-V measurements, it can be seen that the photocurrent increase of the applied bias voltage because of the augmentation of the carrier drift velocity [23]. The ln (I) vs. ln (V) curves are straight lines having different slopes with respect to varying voltage according to the power law relation I α V_r where r is the slope of a line. In the dark current and photocurrent, the linear behavior of curves is indicated the ohmic conduction. The ohmic behavior is very important to the photo sensing because the sensitivity of photodetector can be maximized when the metal-semiconductor junction is ohmic [24].

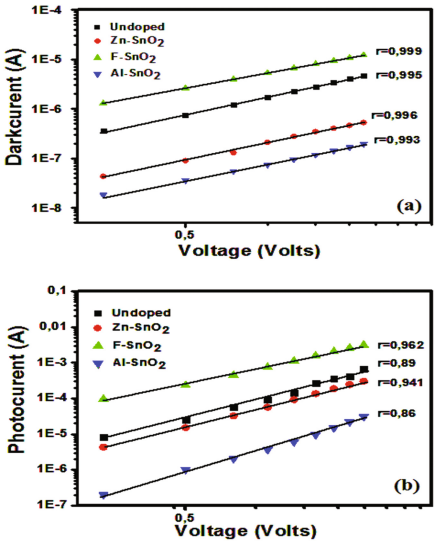

Fig. 3. Variation of (a) dark current and (b) photocurrent as a function of applied voltage of SnO_2 thin films on a logarithmic scale.

3.3.2 UV Detection Mechanism of SnO_2 Thin Films

The photoresponse mechanism of SnO_2 thin films to UV light can be explained in Fig. 4 with according to the following equations:

$$O_2(g) + e^- \rightarrow O_2^- \tag{3}$$

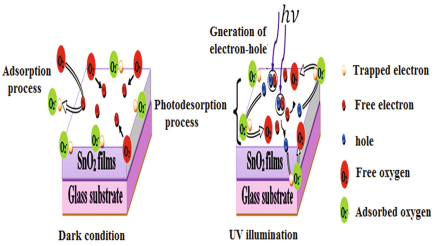

Fig. 4. A schematic of photoresponse mechanism of SnO_2 thin films.

The process of oxygen chemisorptions plays a vital role in UV photoconduction mechanism. Under dark condition, the oxygen molecule O_2 (g) is absorbed on the surface of as negatively charged ions by capturing free electron.

This process leads to the formation of depletion layer near the surface resulting in the bending of the conduction band and valence band, as well as trap center-related band or trap depth. Formation of a large number of ionized oxygen on the thin films surface enhanced the band bending, resulting in a very low conductivity. When the sample is illuminated with UV light, the electron-hole pair is generated by light absorption [25].

The photo-generated hole oxidizes negatively, charged oxygen ions adsorbed on the surface O_2^- (ads). While the remaining unpaired electron in the conduction band increases the conductivity.

$$h\upsilon \rightarrow e^- + h^+ \tag{4}$$

$$h^+ + O_{2\,(ads)}^- \rightarrow O_2(g) \tag{5}$$

3.3.3 Rise and Decay of Photocurrent

The effect of dopant material on the photoconductivity response of SnO_2 thin films under 2 V bias voltages is plotted in Fig. 5, when UV illumination is on, a large increase in the current result and when the illumination is off the current increase gradually, indicating that the films are highly UV sensitive. This figure clearly shows that the SnO_2 thin film based UV photodetector doped with fluorine displayed the maximum photocurrent value.

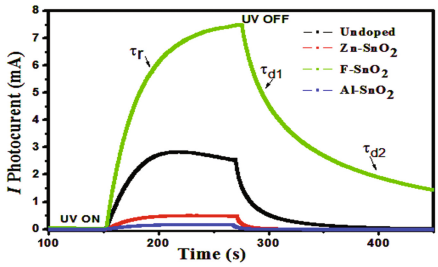

Fig. 5. The rise and recovery-current characteristics of SnO_2 thin films.

The highest on/off ratio was recorded by Al-doped SnO_2 about 5000.

Rise and decay time are estimated by the fitting curve using the exponential functions.

$$I_{ph} = I_0 A \exp^{-t/t_r} \tag{6}$$

$$I_{ph} = I_{ph(\infty)} + A_1 \exp^{-t/t_{d1}} + A_2 \exp^{-t/t_{d2}} \tag{7}$$

The times constants values are noted in Table 2, the minimum values of the rise time and the decay time constants were obtained for the sample doped with aluminum. On other hand, samples doped with fluorine which present a high photocurrent compared to other samples show high rise time and decay time constants.

Table 2. The values of photocurrent, dark current, I_{ON}/I_{OFF} ratio, rise time constant, decay time constants for the thin films.

Samples	I_{light}	I_{dark}	I_{ON}/I_{OFF}	τ_r (s)	τ_{d1} (s)	τ_{d2} (s)
Undoped	2.90×10^{-3}	5.50×10^{-5}	52	27.73	11.18	51.96
F-SnO_2	1.15×10^{-2}	4.90×10^{-4}	23.46	35.71	14.27	83.70
Zn-SnO_2	5.12×10^{-4}	1.77×10^{-6}	289.26	25.60	5.78	30.42
Al-SnO_2	1.78×10^{-4}	3.56×10^{-8}	5000	24.39	4.51	27.63

4 Conclusions

In summary, we have successfully fabricated undoped as well as Zn, Al and F doped SnO_2 UV photodetectors on glass substrates by sol-gel method using low cost dip coating technique. XRD and UV-visible transmission were used to characterize the elaborated films. The results indicated that our thin films show a polycrystalline nature with rutile structure and optical transmittance spectra of the films showed high transparency (>80%) in the visible range and gap energy values were obtained in the range 3.93 to 3.99. In photoconductivity study, the low dark current and high I_{ON}/I_{OFF} current ration with rise time constant τ_r and decay time constants τ_{d1} and τ_{d2} of about

24.39, 4.51 and 27.63 respectively have been obtained for the sample doped with aluminium while the highest I_{ON} current has been obtained for F doped SnO_2 thin films. In this study, it was concluded that the kind of dopant atoms change strongly the performance of UV photodetectors based on SnO_2 thin films.

References

1. Selma, M.H.: Influence of multilayer deposition on characteristics of nanocrystalline SnO_2 thin films produce by Sol-Gel Technique for gas sensor application. Optic **146**, 17–26 (2017)
2. Bu, I.Y.Y.: Sol-gel deposition of fluorine-doped tin oxide glasses for dye sensitized solar cell. Ceram. Int. **40**, 417–422 (2014)
3. Priyadarshini, D.M., Ramanjaneyulu, M., Ramachandra, M.S., Nandita, D.G.: Effect of annealing ambient on SnO_2 thin film transistors. Appl. Surf. Sci. **418**, 414–417 (2016)
4. Rechem, D., Khaial, A., Souifi, A., Djeffal, F.: Effect of annealing time on the performance of tin oxide thin films ultraviolet photodetectors. Thin Solid Films **623**, 1–7 (2017)
5. Khan, A.F., Mazhar, M., Aslam, M., Ashraf, M.: Characterisatics of electron beam evaporated nanocrystalline SnO_2 thin films annealed in air. Appl. Surf. Sci. **256**, 2252–2258 (2010)
6. Kumaril, N., Ghosh, A., Tewari, S., Bhattacharjeel, A.: Synthesis, structural and optical properties of Al doped SnO_2 nanoparticles. Indian J. Phys. **88**, 65–70 (2014)
7. Kucheyev, S.O., Baumann, T.F., Sterne, P.A., Wang, Y.M., Buuren, T., Hamza, A.V., Terminello, L.J., Willey, T.M.: Surface electronic state in three-dimensional SnO_2 nanostructures. Phys. Rev. B **72**(035404), 1–5 (2005)
8. Reddy, A.S., Figueiredo, N.M., Cavaleiro, A.: Nanocrystalline Au: Ag SnO_2 films prepared by pulsed magnetron sputtering. J. Phys. Chem. Solids **74**, 825–829 (2013)
9. Kilic, C., Zunger, A.: Origine of coexistence of conductivity and transparency in SnO_2. Phys. Rev. Lett. **88**(095501), 1–4 (2002)
10. Venkateswara Reddy, P., Venkatramana Reddy, S., Sankra Reddy, B.: Synthesis and properties of (Ni, Al) co-doped nanoparticles. J. Mater. Sci.: Mater. Electron. **27**, 10712–10719 (2016)
11. Liao, M.Y., Sang, L.W., Teraji, T., Imura, M., Alvarez, J., Koide, Y.: Comprehensive investigation of single crystal diamond deep-ultraviolet detectors. J. Appl. Phys. **51**, 090115:1–090115:7 (2012)
12. Sandvik, P., Mi, K., Shahedipour, F., McClintock, R., Yasan, A., Kung, P., Razeghi, M.: $Al_xGa_{1-x}N$ for solar-blind UV detectors. J. Cryst. Growth **231**, 366–370 (2001)
13. Wu, J.M., Kuo, C.H.: Ultaviolet photodetectors made from SnO_2 nanowires. Thin Solid Films **517**, 3870–3873 (2009)
14. Huang, S., Matsubara, K., Cheng, J., Li, H., Pani, W.: Highly enhanced ultraviolet photosensitivity and recovery speed in electrspun Ni-doped SnO_2 nanobelts. Appl. Phys. Lett. **103**(141108), 1–5 (2013)
15. Deng, K., Lu, H., Shi, Z., Liu, Q., Li, L.: Flexible three-dimensional SnO_2 nanowire arrays: atomic layer deposition-assisted synthesis, excellent photodetectors, and field emitters. Appl. Mater. Interfaces **5**, 7845–7851 (2013)
16. Xu, B., Ren, X.R., Gu, G.R., Lan, L.L., Wu, B.J.: Structural and optical properties of Zn-doped SnO_2 films prepared by DC and RF magnetron co-sputtering. Superlattices Microstruct. **89**, 34–42 (2016)

17. Benouis, C.E., Benhaliba, M., Mouffak, Z., Avila-Garcia, A., Tiburcio-Silver, A., Ortega Lopez, M., Romano Trujillo, R., Ocak, Y.S.: The low resistive and transparent Al-doped SnO_2 films: P-type conductivity, nanostructures and photoluminescence. J. Alloys Compd. **603**, 213–223 (2014)
18. Tran, Q.P., Fang, J.S., Chin, T.S.: Properties of fluorine-doped SnO2 thin films by agreen sol–gel method. Mater. Sci. Semicond. Process. **40**, 664–669 (2015)
19. Anandhi, R., Mohan, R., Swaminathan, K., Ravichandran, K.: Influence of aging time of the starting solution on the physical properties of fluorine doped zinc oxide films deposited by a simplified spray pyrolysis technique. Superlattices Microstruct. **51**, 680–689 (2012)
20. Tauc, J., Grigorovici, R., Vancu, A.: Optical properties and electronic structure of amorphous germanium. Phys. Status Solidi B **15**, 627–637 (1966)
21. Ahmed, S.K.F., Khan, S., Ghosh, P.K., Mitra, M.K., Chattopadhyay, K.K.: Effect of Al doping on the conductivity type inversion and electro-optical properties of SnO_2 thin films synthesized by sol-gel technique. Sol-gel Science Technology **39**, 241–247 (2006)
22. Pacheco, A.P., Acosta, D.R., Magana, C.: Effect of the amount of the starting solution on physical properties of SnO_2: F thin films. Surf. Interfaces **6**, 85–90 (2017)
23. Soci, C., Zhang, A., Xiang, B., Dayeh, S.A., Aplin, D.P.R., Park, J., Bao, X.Y., Lo, Y.H., Wang, D.: ZnO nanowire UV photodetectors with high internal gain. Nano Lett. **7**, 1003–1009 (2007)
24. Yoon, Y.J., Park, K.S., Heo, J.H., Park, J.G., Nahm, S., choi, K.J.: Synthesis of $Zn_XCd_{1-X}Se$ (06_X61) alloyed nanowires for variable wave length photodetectors. Mater. Chem. **20**, 2386–2390 (2010)
25. Kim, J.M., Lim, S.J., Nam, T., Kim, D., Kim, H.: The effects of exposure on the device characteristics of atomic layer deposited-ZnO: N thin films transistors. Electrochem. Soc. **158**, 150–154 (2011)